



AFRL-RX-WP-JA-2015-0178

**OPTICAL AND CHEMICAL PROPERTIES OF MIXED-
VALENT RHENIUM OXIDE FILMS SYNTHESIZED BY
REACTIVE DC MAGNETRON SPUTTERING
(POSTPRINT)**

**Neil R. Murphy and John G. Jones
AFRL/RXAP**

**Regina C. Gallagher
Southwestern Ohio Council for Higher Education**

**Lirong Sun
General Dynamics Information Technology**

**John T. Grant
Research Institute, University of Dayton**

**APRIL 2015
Interim Report**

Approved for public release; distribution unlimited.

See additional restrictions described on inside pages

STINFO COPY

**AIR FORCE RESEARCH LABORATORY
MATERIALS AND MANUFACTURING DIRECTORATE
WRIGHT-PATTERSON AIR FORCE BASE, OH 45433-7750
AIR FORCE MATERIEL COMMAND
UNITED STATES AIR FORCE**

NOTICE AND SIGNATURE PAGE

Using Government drawings, specifications, or other data included in this document for any purpose other than Government procurement does not in any way obligate the U.S. Government. The fact that the Government formulated or supplied the drawings, specifications, or other data does not license the holder or any other person or corporation; or convey any rights or permission to manufacture, use, or sell any patented invention that may relate to them.

This report was cleared for public release by the USAF 88th Air Base Wing (88 ABW) Public Affairs Office (PAO) and is available to the general public, including foreign nationals.

Copies may be obtained from the Defense Technical Information Center (DTIC)
(<http://www.dtic.mil>).

AFRL-RX-WP-JA-2015-0178 HAS BEEN REVIEWED AND IS APPROVED FOR
PUBLICATION IN ACCORDANCE WITH ASSIGNED DISTRIBUTION STATEMENT.

//Signature//

NEIL R. MURPHY
Photonic Materials Branch
Functional Materials Division

//Signature//

CHRISTOPHER D. BREWER, Chief
Photonic Materials Branch
Functional Materials Division

//Signature//

KAREN R. OLSON, Actg Chief
Functional Materials Division
Materials and Manufacturing Directorate

This report is published in the interest of scientific and technical information exchange, and its publication does not constitute the Government's approval or disapproval of its ideas or findings.

REPORT DOCUMENTATION PAGE				Form Approved OMB No. 074-0188	
Public reporting burden for this collection of information is estimated to average 1 hour per response, including the time for reviewing instructions, searching existing data sources, gathering and maintaining the data needed, and completing and reviewing this collection of information. Send comments regarding this burden estimate or any other aspect of this collection of information, including suggestions for reducing this burden to Defense, Washington Headquarters Services, Directorate for Information Operations and Reports, 1215 Jefferson Davis Highway, Suite 1204, Arlington, VA 22202-4302. Respondents should be aware that notwithstanding any other provision of law, no person shall be subject to any penalty for failing to comply with a collection of information if it does not display a currently valid OMB control number. PLEASE DO NOT RETURN YOUR FORM TO THE ABOVE ADDRESS.					
1. REPORT DATE (DD-MM-YYYY) April 2015		2. REPORT TYPE Interim		3. DATES COVERED (From – To) 06 May 2010 – 16 March 2015	
4. TITLE AND SUBTITLE OPTICAL AND CHEMICAL PROPERTIES OF MIXED-VALENT RHENIUM OXIDE FILMS SYNTHESIZED BY REACTIVE DC MAGNETRON SPUTTERING (POSTPRINT)				5a. CONTRACT NUMBER In-house	
				5b. GRANT NUMBER	
				5c. PROGRAM ELEMENT NUMBER 62102F	
6. AUTHOR(S) (see back)				5d. PROJECT NUMBER 4348	
				5e. TASK NUMBER	
				5f. WORK UNIT NUMBER X09X	
7. PERFORMING ORGANIZATION NAME(S) AND ADDRESS(ES) (see back)				8. PERFORMING ORGANIZATION REPORT NUMBER	
9. SPONSORING / MONITORING AGENCY NAME(S) AND ADDRESS(ES) Air Force Research Laboratory Materials and Manufacturing Directorate Wright Patterson Air Force Base, OH 45433-7750 Air Force Materiel Command United States Air Force				10. SPONSOR/MONITOR'S ACRONYM(S) AFRL/RXAP	
				11. SPONSOR/MONITOR'S REPORT NUMBER(S) AFRL-RX-WP-JA-2015-0178	
12. DISTRIBUTION / AVAILABILITY STATEMENT Approved for public release; distribution unlimited. This report contains color.					
13. SUPPLEMENTARY NOTES PA Case Number: 88ABW-2014-1633; Clearance Date: 11 April 2014. Journal article published in Optical Materials (2015) 191–196. The U.S. Government is joint author of the work and has the right to use, modify, reproduce, release, perform, display or disclose the work. The final publication is available at http://dx.doi.org/10.1016/j.optmat.2015.03.035 .					
14. ABSTRACT Mixed-valent rhenium oxide thin films were deposited using reactive magnetron sputtering employing a metallic rhenium target within an oxygen–argon environment. The oxygen and argon flow rates were systematically varied, while the extinction coefficient, <i>k</i> , of the deposited layers was monitored using <i>in situ</i> spectroscopic ellipsometry. <i>In situ</i> monitoring was used to identify absorption features specific to ReO ₃ , namely, the minimization of <i>k</i> brought on by the gap between interband absorption features in the UV at 310 nm and the onset of free electron absorption at wavelengths above 540 nm. Based on these results, oxygen flow ratios of 50% and 60% were shown to produce films having optical properties characteristic of ReO ₃ , and thus, were selected for detailed <i>ex situ</i> characterization. Chemical analysis via X-ray photoelectron spectroscopy confirmed that all films consisted largely of ReO ₃ , but had some contributions from Re ₂ O ₃ , ReO ₂ and Re ₂ O ₇ . Additional monitoring of the chemistry, as a function of environmental exposure time, indicated a correlation between structural instability and the presence of Re ₂ O ₃ and Re ₂ O ₇ in the films.					
15. SUBJECT TERMS rhenium oxide, ellipsometry, XPS, thin films, magnetron, sputtering					
16. SECURITY CLASSIFICATION OF:			17. LIMITATION OF ABSTRACT SAR	18. NUMBER OF PAGES 10	19a. NAME OF RESPONSIBLE PERSON (Monitor) Neil R. Murphy
a. REPORT Unclassified	b. ABSTRACT Unclassified	c. THIS PAGE Unclassified			19b. TELEPHONE NUBER (include area code) (937) 255-1829

REPORT DOCUMENTATION PAGE Cont'd

6. AUTHOR(S)

Neil. R. Murphy and John G. Jones - Materials and Manufacturing Directorate, Air Force Research Laboratory
Regina C. Gallagher - Southwestern Ohio Council for Higher Education
Lirong Sun - General Dynamics Information Technology
John T. Grant - Research Institute, University of Dayton

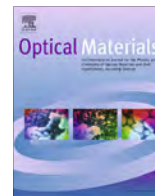
7. PERFORMING ORGANIZATION NAME(S) AND ADDRESS(ES)

AFRL/RXAP
Air Force Research Laboratory
Materials and Manufacturing Directorate
Wright-Patterson Air Force Base, OH 45433-7750

Southwestern Ohio Council for Higher Education
3155 Research Blvd., Suite 204
Dayton, OH 45420

General Dynamics Information Technology
5100 Springfield Street
Dayton, OH 45433

Research Institute, University of Dayton
300 College Park
Dayton, OH 45469



Optical and chemical properties of mixed-valent rhenium oxide films synthesized by reactive DC magnetron sputtering



Neil R. Murphy^{a,*}, Regina C. Gallagher^b, Lirong Sun^c, John G. Jones^a, John T. Grant^{c,d}

^a Air Force Research Laboratory, Materials and Manufacturing Directorate, Wright-Patterson Air Force Base (WPAFB), Dayton, OH 45433, USA

^b Southwestern Ohio Council for Higher Education, 3155 Research Blvd., Suite 204, Dayton, OH 45420, USA

^c General Dynamics Information Technology, 5100 Springfield Street, Dayton, OH 45431, USA

^d Research Institute, University of Dayton, 300 College Park, Dayton, OH 45469, USA

ARTICLE INFO

Article history:

Received 20 January 2015

Accepted 16 March 2015

Available online 3 April 2015

Keywords:

Rhenium oxide

Ellipsometry

XPS

Thin films

Magnetron

Sputtering

ABSTRACT

Mixed-valent rhenium oxide thin films were deposited using reactive magnetron sputtering employing a metallic rhenium target within an oxygen–argon environment. The oxygen and argon flow rates were systematically varied, while the extinction coefficient, k , of the deposited layers was monitored using *in situ* spectroscopic ellipsometry. *In situ* monitoring was used to identify absorption features specific to ReO_3 , namely, the minimization of k brought on by the gap between interband absorption features in the UV at 310 nm and the onset of free electron absorption at wavelengths above 540 nm. Based on these results, oxygen flow ratios of 50% and 60% were shown to produce films having optical properties characteristic of ReO_3 , and thus, were selected for detailed *ex situ* characterization. Chemical analysis via X-ray photoelectron spectroscopy confirmed that all films consisted largely of ReO_3 , but had some contributions from Re_2O_3 , ReO_2 and Re_2O_7 . Additional monitoring of the chemistry, as a function of environmental exposure time, indicated a correlation between structural instability and the presence of Re_2O_3 and Re_2O_7 in the films.

Published by Elsevier B.V.

1. Introduction

Rhenium, a hexagonally close packed refractory metal, has several oxides with a variety of interesting optical and electronic properties. The commonly occurring oxides of rhenium are ReO_2 , ReO_3 , and Re_2O_7 [1–7]. The lowest valence oxide, ReO_2 , is monoclinic in structure, while ReO_3 consists of a network of ReO_6 octahedra having a cubic, “perovskite-type” structure [4,8]. Finally, Re_2O_7 consists of ReO_6 octahedra and ReO_4 tetrahedra, and has been reported to be highly hygroscopic, decomposing into perrhenic acid (HReO_4) upon exposure to moisture [1,3,9,10]. The most widely investigated of these compounds is ReO_3 , due to its metallic-like conductivity and its low absorption within the visible spectrum, both of which are similar to silver [4,11–13]. The high conductivity $\sigma_{\text{ReO}_3} = 10^3\text{--}10^4 (\Omega \text{ cm})^{-1}$ [9,12] and minimal optical absorption are a direct consequence of the electronic configuration of ReO_3 , which contains a single free electron within the 5d electron shell [4,8,12,14]. As a result of their unique optical and

electronic properties, thin films of ReO_3 have been used for several diverse applications, including catalysis [10,15–18], interfacial layers for high T_c superconductors [9], anode buffer layers for polymer solar cells [7], and electrical contacts for liquid crystal devices [8]. Additionally, ReO_3 has ultraviolet (UV) absorption features centered at 310, 177, 155, 124 nm (4, 7, 8 and 10 eV), as well as the onset of free-electron absorption at 540 nm (2.3 eV) [4,12,13]. Interestingly, there are no dominant absorption features between 310 and 540 nm (2.3–4 eV), giving rise to a small transmission window within the visible region. Therefore, thin films of ReO_3 could also have promise as a transparent-conductive material in applications requiring a narrow transmission band.

Deposition of mixed-valent rhenium oxide thin films has been performed using radio-frequency (RF) magnetron sputtering [9], electrodeposition [5–7,19,20], evaporation from rhenium filaments [1], and reactive direct current magnetron sputtering (DCMS) [4]. At this time, there have been very few studies on the optical and chemical properties of rhenium–oxygen compounds deposited using reactive DCMS [4], which is the subject of this work. Work by Ghanashyam Krishna et al. has described a method of depositing rhenium–oxygen compounds using reactive DCMS, wherein the bias voltage was varied and its effect on the spectral reflectivity was systematically analyzed [4]. Results obtained by Ghanashyam

* Corresponding author at: Air Force Research Laboratory, Materials & Manufacturing Directorate, 3005 Hobson Way, Wright-Patterson AFB, OH 45433, USA. Tel.: +1 937 255 1829.

E-mail address: neil.murphy.1@us.af.mil (N.R. Murphy).

Krishna et al. indicate that it is possible to use reactive DCMS to deposit 50–180 nm thin films that demonstrate optical behavior analogous to bulk ReO_3 , as reported by Weaver et al. [12] and Feinlieb et al. [12]. However, to our knowledge, there are currently no studies reporting on the relationship between the chemistry and spectral (380–1700 nm) optical properties of mixed-valent rhenium oxide thin films deposited via reactive DCMS.

Within this study we devise a method of maximizing the ReO_3 content within the films using *in situ* spectroscopic ellipsometry (iSE). *In situ* monitoring of the optical behavior, throughout film growth, allows for the selection of oxygen (Q_{O_2}) and argon (Q_{Ar}) flow rates capable of increasing ReO_3 content within the films. Process optimization was achieved through real-time identification of characteristic absorption features, namely the minimization of the extinction coefficient, k , at wavelengths between 450 and 750 nm (1.65–2.75 eV). After establishing the deposition conditions required for maximizing ReO_3 content in the films, analyses of their chemical compositions and their oxidation states, were performed using X-ray photoelectron spectroscopy (XPS). In addition to XPS, X-ray reflectivity (XRR) was used to measure the film thickness and density. These XPS and XRR measurements, as well as additional SE measurements, were made *ex situ* after one and thirty days exposure to atmosphere at ambient temperatures of 20–25 °C and relative humidity between 20% and 25%. Based on the aforementioned reports of instability [1,3,9,10], it is important to analyze environmental robustness prior to using ReO_3 thin films for applications requiring consistent optical performance and structural stability.

2. Materials and methods

2.1. Deposition

Rhenium oxide thin films were deposited within a stainless steel high vacuum chamber evacuated to a pressure of 5.3×10^{-5} Pa (4×10^{-7} Torr). A 3 mm thick, 50 mm diameter rhenium sputter target (99.99%, K.J. Lesker), was magnetically attached to a 50 mm magnetron source (MeiVac, MAK) at an angle of 20° with respect to the substrate normal. The distance between the target and the p-type silicon (100) (University Wafer LLC) substrate was 9 cm. During deposition, research grade O_2 (99.995%) and Ar (99.999%) were introduced via separate mass flow controllers, mixed prior to entering the chamber, and maintained at a total pressure of 1.33 Pa (10 mTorr) at a pumping speed of 25 L/s [21]. Oxygen and argon content were regulated by controlling the flow rates Q_{O_2} and Q_{Ar} , while the total flow rate Q_{TOT} was kept constant at 20 sccm. The oxygen fraction f_{O_2} , represented by $Q_{\text{O}_2}/Q_{\text{TOT}}$, was varied from $f_{\text{O}_2} = 0.0$ –0.8 by increments of 0.1, while the optical constants were monitored every ten seconds using *in situ* spectroscopic ellipsometry. *In situ* data were gathered during continuous deposition for a period of one minute at each increment of f_{O_2} . Values of f_{O_2} resulting in film layers with minimal extinction coefficients throughout the visible region ($400 \leq \lambda \leq 750$ nm) were selected and used in the deposition of multiple films for further *ex situ* analysis. The films selected for *ex situ* optical and chemical analysis were deposited for three minutes at a cathode voltage $V_c = 631$ V and current $I_c = 80$ mA, resulting in an applied power of 50 W. Depositions took place upon a substrate platen set to rotate at 12 RPM to mitigate the anisotropy imparted by the sputtering process. Note that no heating, outside of thermal contributions from the plasma, was applied to the substrate.

2.2. Characterization

The optical constants of the rhenium oxide films were measured using a J.A. Woollam M2000VI spectroscopic ellipsometer

(SE) at an angle of incidence of 70°, near the Brewster's angle for silicon. The extinction coefficient (k) and the refractive index (n) were obtained upon fitting the raw polarization data to the Kramer's Kronig consistent model described within Section 3.4. Thickness values obtained through spectroscopic ellipsometry were verified using a KLA-Tencor stylus profilometer.

XPS was performed using a Physical Electronics 5700 equipped with an Al K α X-ray source operating at 1486.6 eV. The energy scale was calibrated using Au and Cu, according to the procedures outlined by the ISO Standard, ISO 15472. Survey scans were acquired at an analyzer pass energy of 187.85 eV (0.80 eV energy step) while high energy resolution scans of the core level Re 4f, Re 4s, C 1s, and O 1s transitions were acquired at a pass energy of 29.35 eV (0.125 eV energy step). High energy resolution spectra were calibrated with respect to the Re 4f $_{7/2}$ transition, corresponding to the Re^{6+} valence state, at a binding energy of 44.9 (± 0.1) eV, as reported by Tysoe et al. [1]. This reference energy was used for all films in order to allow for any small electrical charging. To mitigate the level of error present in peak fittings, the spacing between the 4f $_{5/2}$ and 4f $_{7/2}$ components was constrained to reflect spin-orbit splitting of 2.5 eV [22]. Additionally, the components of the 4f doublets were fit using equal full-width half-maximum values, as well as area ratios of 3:4 (4f $_{5/2}$:4f $_{7/2}$) [19]. Shirley background subtraction and 70% Gaussian 30% Lorentzian line shapes were used to fit all spectra within the CasaXPS 2.3.16 software package [23]. To obtain a metallic reference for use in quantifying binding energy shifts, some samples were sputtered for 5 min using a differentially pumped ion gun at 4 keV with an argon pressure of 10×10^{-3} Pa and an emission current of 25 mA. The binding energy obtained for the metallic Re^0 4f $_{7/2}$ peak was 40.3 eV. Note that no sputtering was utilized prior to analysis of survey and high resolution scans due to the facile reduction of higher order rhenium–oxygen compounds during sputtering [24,25].

Electron micrographs were taken using an FEI Sirion scanning electron microscope (SEM). Measurements of the films' densities were performed via X-ray reflectivity analysis (XRR) using a Rigaku Smartlab X-ray diffractometer, while grazing incidence X-ray diffraction (GIXRD) was also performed, indicating that all films deposited were amorphous. The observation of the films' amorphous character is in line with results obtained by Hahn et al. for cathodically electrodeposited ReO_3 thin films [6]. In the absence of crystalline character related to various rhenium–oxygen coordination compounds, establishment of the presence of individual compounds was performed through careful analysis of relative charge shifts present within high energy resolution XPS spectra. Further corroboration of the presence of specific compounds, namely ReO_3 , was performed through comparison of SE data with data presented within the literature.

3. Results and discussion

3.1. *In situ* monitoring of optical constants

In situ ellipsometry measurement of rhenium oxide as a function of increasing oxygen content was used in order to determine the oxygen fraction required to minimize the k within the visible region ($400 \leq \lambda \leq 750$ nm). Since oxides of rhenium are not dielectric, like many transition metal oxides, the onset of arcing and process instability as a function of increasing f_{O_2} was not an issue. As shown in Fig. 1, values of k at 450, 600 and 750 nm, are consistent with reported values for metallic rhenium at $f_{\text{O}_2} = 0.0$ [26]. As f_{O_2} is increased, k values continue to decrease until reaching $f_{\text{O}_2} = 0.4$, where a slight increase in k occurs as the potential result of the onset of absorption features related to lower valent rhenium species [20]. As f_{O_2} increases, to 0.5 and 0.6, the target surface begins

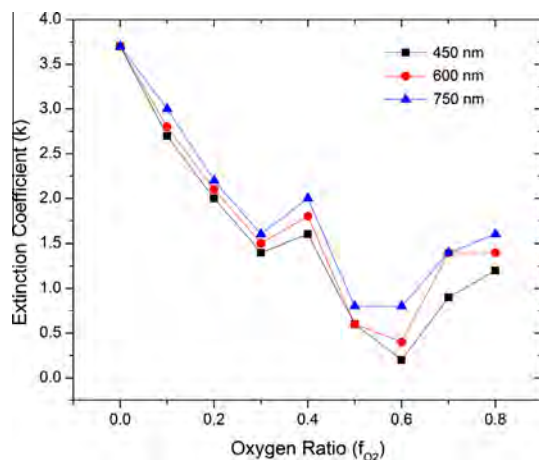


Fig. 1. Extinction coefficient values as a function of oxygen flow rate, f_{O_2} , at 450, 600, and 750 nm wavelengths.

to become increasingly coated with adsorbed oxygen, corresponding to a deposition environment conducive to the growth of ReO_3 , as evinced by the characteristic reduction in k between 450 and 750 nm [4,12,13]. Further increases in f_{O_2} , to 0.7 and above, lead to larger values of k . The observed increases in k at $f_{O_2} > 0.6$ are likely due to the formation of Re_2O_7 , however, further work would be necessary to quantify the optical behavior of Re_2O_7 within this region. For depositions taking place at $f_{O_2} \geq 0.2$, the k minima occur near 450 nm, with the lowest values, 0.2 and 0.6, corresponding to $f_{O_2} = 0.6$ and 0.5, respectively. Diffuse reflectance studies of bulk, single crystal ReO_3 performed by Weaver et al. [13] and Feinleib et al. [12] reported values of $k_{450 \text{ nm}} = 0.0$ and 0.2, respectively. Despite differences in morphology and crystallinity, good agreement exists between the *in situ* optical constants obtained at $f_{O_2} = 0.6$ and reported values [12,13]. Therefore, rhenium oxide thin films were subsequently deposited at $f_{O_2} = 0.5$ and 0.6 and characterized extensively using SEM, XRR, XPS and SE, as discussed below.

3.2. Microstructural characterization

Secondary electron micrographs of rhenium oxide films deposited at $f_{O_2} = 0.5$ and $f_{O_2} = 0.6$ are shown in Fig. 2 after 30 days air exposure. The microstructure of the film deposited at $f_{O_2} = 0.5$ shows a dendritic structure dotted with dark features that appear to be in the form of droplets (Fig. 1a, inset). Rhenium oxide deposited at $f_{O_2} = 0.6$ (Fig. 1b) is shown to contain a large, interconnected network of cracks. These cracks appear to be a consequence of buckling induced by compressive stress as a result of the volumetric expansion of the film (Fig. 2a, inset). Expansion and droplet formation are thought to be the result of the instability of Re_2O_7 ($\rho = 6.10 \text{ g/cm}^3$), forming HReO_4 ($\rho = 2.15 \text{ g/cm}^3$) upon exposure to moisture [3,27]. The films' non-uniform microstructure and poor adhesion are similar to reports of instability associated with the presence of Re_2O_7 and perrenic acid, HReO_4 [1,3,6,8,9,27].

XRR, described in detail by Ferrari et al. [28], was utilized to calculate the density of the rhenium oxide films after 1 day and 30 days of atmospheric exposure. Due to the high levels of macro-segregation, and the resulting non-uniform surface morphology, XRR analysis was limited to the calculation of density by measurement of the total reflection, or critical angle [28]. Films deposited at $f_{O_2} = 0.6$ were shown to retain their initial density of 5.2 g/cm^3 , while films deposited at $f_{O_2} = 0.5$ showed an average density reduction from 5.0 to 3.8 g/cm^3 . Typical densities for rhenium oxides range from 11.4 g/cm^3 for ReO_2 to 6.10 g/cm^3

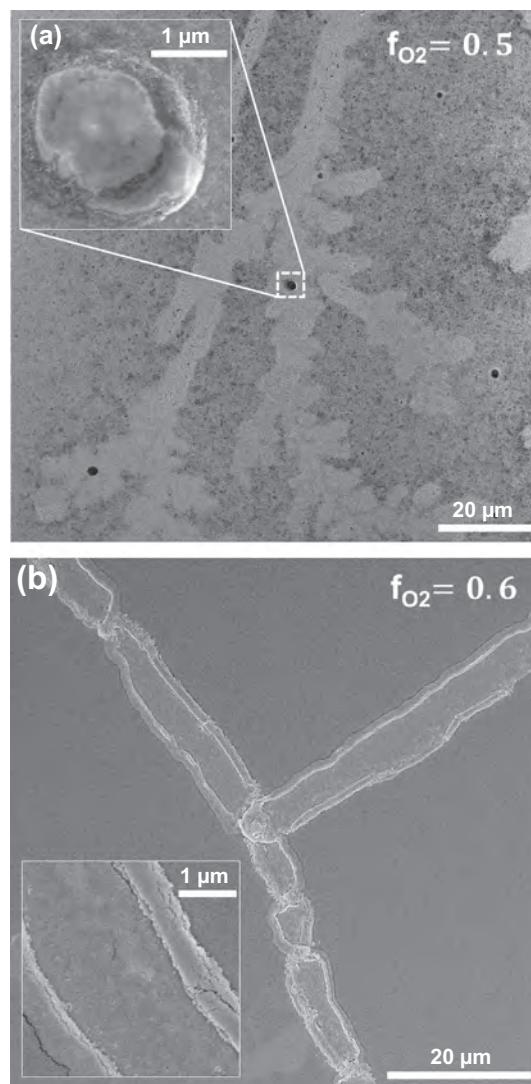


Fig. 2. Scanning electron micrographs for rhenium oxide films deposited at oxygen fractions (a) $f_{O_2} = 0.5$ and (b) 0.6.

for Re_2O_7 [3,27]. Density values far below the relatively low density of Re_2O_7 are indicative of the presence of much lower density HReO_4 . Thickness measurements via SE for $f_{O_2} = 0.5$ show a thickness increase from $80 (\pm 10) \text{ nm}$ *in vacuo* to $150 (\pm 20) \text{ nm}$, after 30 days air exposure. Films deposited at $f_{O_2} = 0.6$ were $90 (\pm 7) \text{ nm}$ thick *in vacuo* and $93 (\pm 7) \text{ nm}$ after 30 days air exposure, essentially unchanged. Despite microstructural non-uniformity, thickness changes for $f_{O_2} = 0.5$ measured by ellipsometry correlate to volumetric expansion related to their density reduction after 30 days.

3.3. Surface analysis

The compositions and chemical states of the rhenium oxide films, measured using XPS, demonstrated marked changes as a result of environmental exposure. Survey (Fig. 3) and high-resolution (Fig. 4) scans were acquired for films deposited at $f_{O_2} = 0.5$ and 0.6 after exposure to air for 1 and 30 days. The initial survey scan of the film deposited at $f_{O_2} = 0.5$ after 1 day of exposure showed a composition of 30% Re, and 70% O, with negligible amounts of adventitious carbon. After 30 days exposure to air, the $f_{O_2} = 0.5$ film was found to have a surface composition of 25% Re, 64% O, and 11% C. The compositions of rhenium oxide deposited

at $f_{O_2} = 0.6$, following air exposures of 1 and 30 days changed from 30% to 27% Re, 70% to 65% O, and 0% to 8% C, respectively. Note that the atomic compositions were similar after 1 day air exposure, but

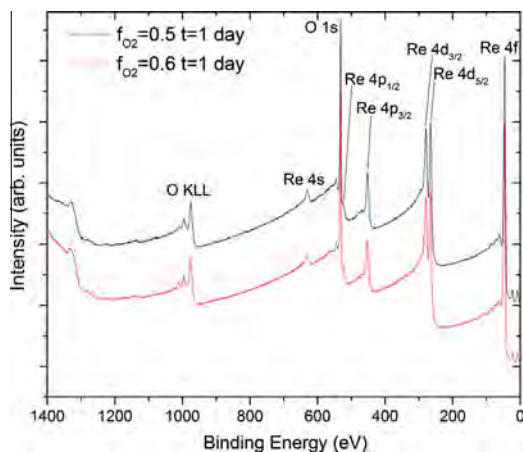


Fig. 3. XPS survey scans used for composition measurement for films deposited at $f_{O_2} = 0.5$ and 0.6 after 1 day air exposure.

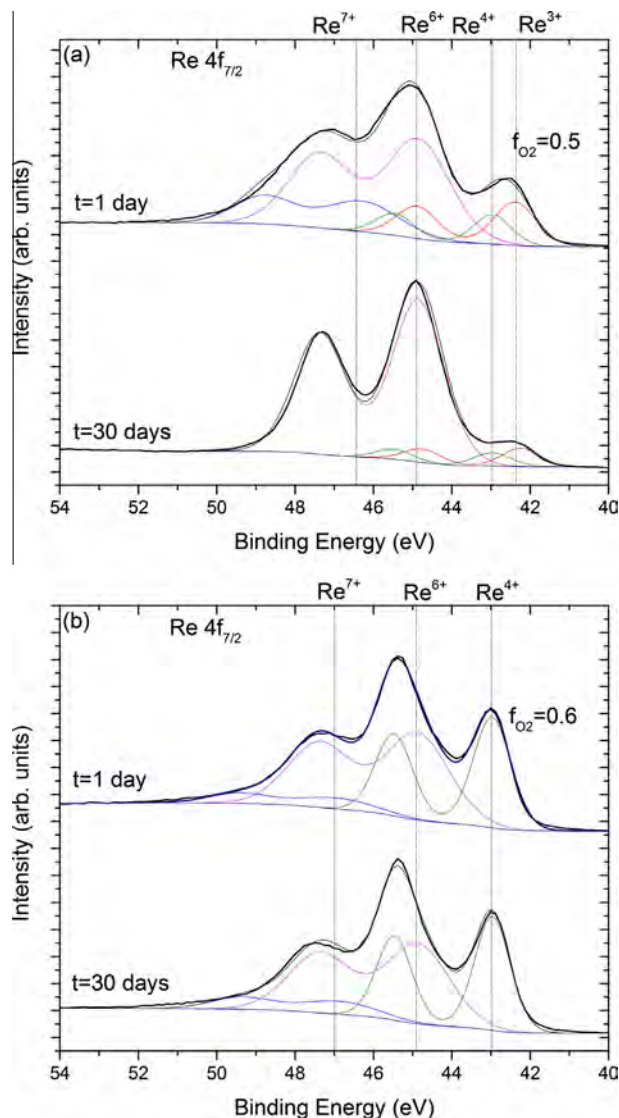
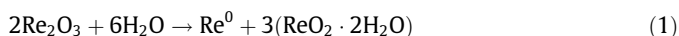


Fig. 4. High resolution XPS spectra of the Re 4f transitions after 1 and 30 days air exposure for films deposited at (a) $f_{O_2} = 0.5$ and (b) 0.6 . Spectra are offset for clarity.

as discussed below, their rhenium oxidation states are very different.

High resolution XPS (Fig. 4), performed after 1 day of air exposure, indicated that all films deposited were found to contain 4f transitions with binding energies corresponding valence states of Re^{4+} , Re^{6+} , Re^{7+} , for their respective compounds: ReO_2 , ReO_3 , and Re_2O_7 [1,18,29]. In addition to these compounds, films deposited at $f_{O_2} = 0.5$ were found to contain up to 15% of the Re^{3+} valence state. The presence of the Re^{3+} valence state, and its corresponding oxide, Re_2O_3 , has been reported previously in the literature [6,25,30,31]. Interestingly, Re_2O_3 has been reported to undergo catalytic disproportionation in the presence of moisture, decomposing into metallic Re^0 and hydrous ReO_2 , as described in Eq. (1) [6,30,31]:



Binding energies corresponding to the Re $4f_{7/2}$ transitions are shown within Table 1. The chemical state distribution measured for $f_{O_2} = 0.5$ (Fig. 4a) after 1 day air exposure consists of 15% Re^{3+} , 10% Re^{4+} , 55% Re^{6+} , and 20% Re^{7+} . After air exposure for $t = 30$ days (Fig. 4a), the surface chemistry is 7% Re^{3+} , 5% Re^{4+} , 88% Re^{6+} , and 0% Re^{7+} . Given the reported instability of both Re_2O_3 and Re_2O_7 in the presence of moisture [1,3,6,8,9,27], it is possible that both hydrous ReO_2 and liquid $HReO_4$, could have formed during environmental exposure and subsequently evaporated under the UHV conditions within the XPS instrument. Tysoe, et al., have reported similar losses of rhenium species, correlated to the presence of Re_2O_7 [1]. Films deposited at $f_{O_2} = 0.6$ (Fig. 4b) were found to contain 40% Re^{4+} , 53% Re^{6+} , and 7% Re^{7+} after 1 day, and 40% Re^{4+} , 50% Re^{6+} , and 10% Re^{7+} after 30 days, exhibiting very little change as a result of environmental exposure. Therefore, according to the XPS results, the surface chemistry of films grown at $f_{O_2} = 0.6$

Table 1

Re $4f_{7/2}$ binding energies measured from curve fitted data for $f_{O_2} = 0.5$ and 0.6 .

Oxidation state	Re $4f_{7/2}$ binding energy (eV)	
	$f_{O_2} = 0.5$	$f_{O_2} = 0.6$
3+	42.4	–
4+	42.9	42.9
6+	44.9	44.9
7+	46.4	46.9

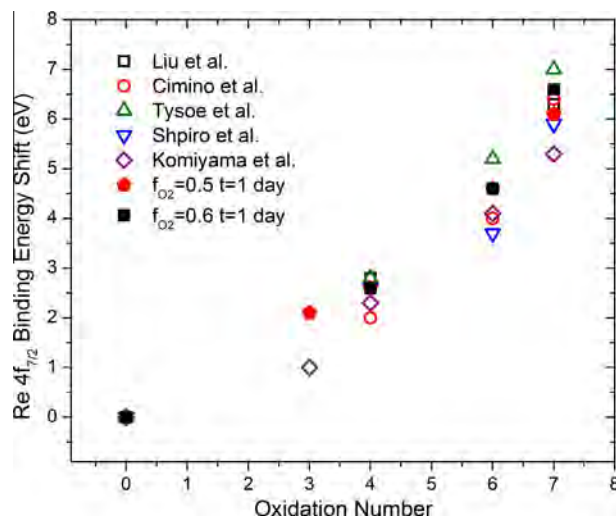


Fig. 5. Plot of the binding energy shift for the Re $4f_{7/2}$ peak as a function of oxidation state, as compared to results obtained by Liu et al. [32], Cimino et al. [29], Tysoe et al. [1], Shpiro et al. [35], and Komiyama et al. [25].

remained relatively stable, while films grown at $f_{O_2} = 0.5$ demonstrated large changes after 30 days exposure to air.

Given the uncertainty inherent in the peak fitting process, comparisons were made between high energy resolution XPS data obtained for films deposited at $f_{O_2} = 0.5$ and 0.6, and those analyzed within the literature [6,25,29,32]. In addition to probing the accuracy of the fitting process, the comparisons shown in Fig. 5 help to identify potential trends in peak location as a function of oxidation state. Identification of known binding energy shifts is especially helpful for the validation of the presence of the unstable Re^{3+} oxidation state. Typically, as a result of increases in binding energy brought on by oxygen bonding, the binding energy will increase almost linearly as a function of oxidation number. A similar observed trend for rhenium has been noted elsewhere by Komiyama et al. [25]. The binding energies of the Re 4f_{7/2} peaks obtained within this study are in good agreement with reported values, as seen in Fig. 5.

3.4. Optical properties

Detailed spectroscopic ellipsometry analysis of the rhenium oxide thin films was conducted *in vacuo* for films grown at $f_{O_2} = 0.5$ and 0.6. The measurements were made over a wavelength

Table 2
General oscillator parameters and error estimates used for fitting ellipsometry data.

f_{O_2}	t (days)	Amplitude	Broadening	Center energy (eV)	Thickness (nm)	MSE
0.5	0	3.3 ± 0.3	0.54 ± 0.01	3.42 ± 0.01	79	5.2
		10 ± 1	3.76 ± 0.05	0.70 ± 0.06		
	1	3.3 ± 0.1	0.54 ± 0.01	3.42 ± 0.01	79	5.1
		10 ± 1	3.77 ± 0.04	0.71 ± 0.06		
	30	0.4 ± 0.1	0.45 ± 0.03	2.80 ± 0.01	150	15.6
0.6	0	2.2 ± 0.1	1.25 ± 0.01	1.68 ± 0.01		
		12 ± 1	0.44 ± 0.04	4.5 ± 0.1		
	1	35 ± 1	0.85 ± 0.01	0.58 ± 0.01	90	8.9
		2.8 ± 0.1	0.53 ± 0.01	3.30 ± 0.01		
	30	28 ± 1	0.91 ± 0.01	0.63 ± 0.01	89	10.3
		2.8 ± 0.1	0.53 ± 0.01	3.33 ± 0.01		
		39 ± 2	0.73 ± 0.01	0.64 ± 0.01	93	22.5
		1.9 ± 0.1	0.49 ± 0.02	3.27 ± 0.01		

range of 380–1700 nm. The resulting magnitude (ψ) and phase difference (Δ) information obtained from the two samples was then parameterized using two Lorentz oscillator models, as described elsewhere by Jellison [33]. Multiple oscillators were required due to the fact that ReO_3 facilitates absorption via interband transitions at $\lambda < 540$ nm ($h\nu > 2.3$ eV) specifically the tail of the absorption feature centered at 310 nm (4 eV) as the other interband absorption features are out of the range of ellipsometer used for these measurements. Additional absorption features accounted for within the model include free-electron, or intraband transitions beginning at $\lambda = 540$ nm and increasing into the NIR and IR ($h\nu < 2.3$ eV) [4,6,12,13]. Oscillator parameters, error estimates, and goodness-of-fit data can be found within Table 2. Fig. 6a shows both the refractive index and extinction coefficient values at different exposure times. For $f_{O_2} = 0.6$, initial and prolonged exposure to atmosphere have very little effect on the optical properties. Free electron absorption within the near infrared region is parameterized using a Lorentz oscillator centered at 1940 nm (0.64 eV) the corresponding extinction coefficients and refractive indices are shown to increase alongside wavelength, as expected in the case of intraband transitions [34]. Interband transitions were measured at 375 nm (3.3 eV), close to the known ReO_3 absorption band at 310 nm (4.0 eV); discrepancies between these two values are likely due to the fact that the ellipsometer is currently not equipped to exceed 380 nm (3.25 eV). Note that ReO_3 undergoes additional interband transitions at 177, 155, 124 and 89 nm (7, 8, 10 and 14 eV) [4,12,13], while Re_2O_7 has absorption bands at 310 and 240 nm (4.0 and 5.2 eV) [4,10]. Therefore, it will be difficult to determine if absorption occurring at or near 310 nm (4 eV) is characteristic of either compound. In the case of films deposited at $f_{O_2} = 0.5$, the initial optical behavior is similar to the $f_{O_2} = 0.6$ films, experiencing interband transitions near 375 nm (3.3 eV), with intraband absorption occurring above 540 nm (2.3 eV), centered at 1900 nm (0.65 eV). Films deposited at $f_{O_2} = 0.5$ demonstrate little change upon initial exposure to atmosphere, however, the optical properties are shown to have rapidly degraded after 30 days air exposure. These films no longer demonstrate the characteristic free electron absorption associated with ReO_3 , instead they have a very low extinction coefficient, less than 0.7 from

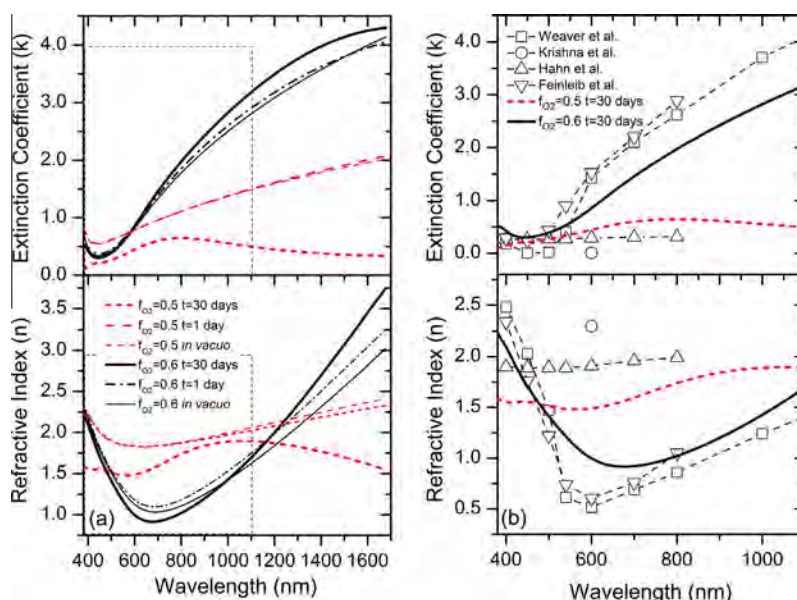


Fig. 6. Optical constants (n , k) obtained for mixed valent rhenium oxide thin films from 380 to 1700 nm, part (a). Note that both refractive index and extinction coefficient values for films deposited at $f_{O_2} = 0.5$ *in vacuo* (thin dashed) and after 1 day exposure (dotted) overlap one another significantly. The 30 day data within the dashed boxes in part (a) are expanded and shown within part (b), along with comparisons to reported values by Feinleib et al. [12], Weaver et al. [13], Ghanashyam Krishna et al. [4] and Hahn et al. [6].

380 to 1700 nm. In addition, the $f_{O_2} = 0.5$ film required three Lorentz oscillators to accommodate absorption bands at 443, 752 and 295 nm (2.8, 1.65 and 4.2 eV). These films demonstrate similar optical behavior to highly oxidized, solution deposited rhenium oxide compounds obtained by Hahn et al. [6] as shown in Fig. 6b. Additional comparisons between films deposited at $f_{O_2} = 0.6$ and results obtained by Feinleib et al. [12] and Weaver et al. [13], for single crystal ReO_3 , can be seen in Fig. 6b, where our data indicates reasonably similar optical behavior to their bulk single crystals.

4. Conclusions

Despite having only a 10% difference in f_{O_2} values, rhenium oxide films deposited at $f_{O_2} = 0.5$ and 0.6 have disparate optical and chemical properties, especially as a function of environmental exposure time. While films deposited under both conditions are composed of similar proportions of rhenium to oxygen, 70% O and 30% Re, as calculated via XPS, their chemistries are quite different. The main difference between the oxide species present in films deposited at $f_{O_2} = 0.5$ and 0.6 is the existence of Re^{3+} associated with an oxygen fraction of 0.5. Films containing the Re^{3+} valence state, a result of the lower oxygen fraction used during growth, have demonstrated large decreases in density, droplet formation, poor adhesion, and rapid degradation of optical performance. Similarly, films deposited at $f_{O_2} = 0.6$ have shown poor adhesion, and slight microstructural instability in the form of compressive-mode cracking. However, films deposited at $f_{O_2} = 0.6$ have demonstrated very small changes in their optical and chemical properties as a function of environmental exposure. The poor adhesion and microstructural instability of the mixed valent rhenium oxide films within this study is consistent with other reports of moisture related degradation. Despite the structural implications associated with exposure to moisture, films deposited at an oxygen level sufficient to preclude the formation of Re^{3+} were able to retain their optical and chemical properties throughout the 30 day exposure period.

References

- [1] W. Tysoe, F. Zaera, G. Somorjai, *Surf. Sci.* 200 (1988) 1–14.
- [2] W. Jeitschko, A. Sleight, *J. Solid State Chem.* 4 (1972) 324–330.
- [3] C.T. Sims, C.M. Craighead, R.I. Jaffee, D.N. Gideon, E.N. Wyler, F.C. Todd, D.M. Rosenbaum, E.M. Sherwood, I.E. Campbell, Defense Technical Information Center WADC TR-54-371, 1954.
- [4] M. Ghanashyam Krishna, A. Bhattacharya, *Solid State Commun.* 116 (2000) 637–641.
- [5] A.V. Uscategui, E. Mosquera, L. Cifuentes, *Mater. Lett.* 94 (2012) 44–46.
- [6] B.P. Hahn, R.A. May, K.J. Stevenson, *Langmuir* 23 (2007) 10837–10845.
- [7] Z. Tan, L. Li, F. Wang, Q. Xu, S. Li, G. Sun, X. Tu, X. Hou, J. Hou, Y. Li, *Adv. Energy Mater.* 4 (2013) 1300884.
- [8] E. Cazzanelli, M. Castriota, S. Marino, N. Scaramuzza, J. Purans, A. Kuzmin, R. Kalendarev, G. Mariotto, G. Das, *J. Appl. Phys.* 105 (2009) 114904–114907.
- [9] K. Jiao, L. Chang, R. Wallace, W. Anderson, *Appl. Supercond.* 3 (1995) 55–60.
- [10] L. Wang, W.K. Hall, *J. Catal.* 82 (1983) 177–184.
- [11] H. Ehrenreich, H. Philipp, *Phys. Rev.* 128 (1962) 1622.
- [12] J. Feinleib, W. Scouler, A. Ferretti, *Phys. Rev.* 165 (1968) 765.
- [13] J. Weaver, D. Lynch, *Phys. Rev. B* 6 (1972) 3620.
- [14] C. Granqvist, *Sol. Cells* 32 (1994) 369–382.
- [15] R.M. Edreva-Kardjieva, M.A. Vuurman, J.C. Mol, *J. Mol. Catal.* 76 (1992) 297–305.
- [16] M. Vuurman, D. Stufkens, A. Oskam, I. Wachs, *J. Mol. Catal.* 76 (1992) 263–285.
- [17] F.D. Hardcastle, I.E. Wachs, J.A. Horsley, G.H. Via, *J. Mol. Catal.* 46 (1988) 15–36.
- [18] J. Okal, *Appl. Catal. A* 287 (2005) 214–220.
- [19] R. Schrebler, P. Cury, C. Suárez, E. Muñoz, F. Vera, R. Córdova, H. Gómez, J. Ramos-Barrado, D. Leinen, E. Dalchiele, *Thin Solid Films* 483 (2005) 50–59.
- [20] J. Zerbino, A. Luna Castro, C. Zinola, E. Méndez, M. Martins, *J. Electroanal. Chem.* 521 (2002) 168–174.
- [21] S. Berg, T. Nyberg, *Thin Solid Films* 476 (2005) 215–230.
- [22] J.F. Moulder, J. Chastain, R.C. King, *Handbook of X-Ray Photoelectron Spectroscopy: A Reference Book of Standard Spectra for Identification and Interpretation of XPS Data*, Physical Electronics Eden Prairie, MN, 1995.
- [23] Neal Fairley, Casa Software Ltd., CasaXPS Version 2.3.16 1999–2011.
- [24] K. Kim, N. Winograd, *Surf. Sci.* 43 (1974) 625–643.
- [25] M. Komiyama, Y. Ogino, Y. Akai, M. Goto, *J. Chem. Soc., Faraday Trans. 2* (79) (1983) 1719–1728.
- [26] R.B. Zipin, *J. Opt. Soc. Am.* 56 (1966) 1543–1543.
- [27] D.R. Lide, *CRC Handbook of Chemistry and Physics 2004–2005: A Ready-Reference Book of Chemical and Physical Data*, CRC Press, Boca Raton, FL, 2004.
- [28] A. Ferrari, A. Libassi, B. Tanner, V. Stolojan, J. Yuan, L. Brown, S. Rodil, B. Kleinsorge, J. Robertson, *Phys. Rev. B* 62 (2000) 11089.
- [29] A. Cimino, D. Gazzoli, G. Minelli, M. Valigi, *Z. Anorg. Allg. Chem.* 494 (1982) 207–218.
- [30] R. Busey, E. Sprague, R. Bevan Jr, *J. Phys. Chem.* 73 (1969) 1039–1042.
- [31] E. Méndez, M.F. Cerdá, A.M. Castro Luna, C.F. Zinola, C. Kremer, M.E. Martins, *J. Colloid Interface Sci.* 263 (2003) 119–132.
- [32] P. Liu, D.K. Shuh, *J. Electron Spectrosc. Relat. Phenom.* 114 (2001) 319–325.
- [33] G.E. Jellison, *Thin Solid Films* 234 (1993) 416–422.
- [34] J.I. Pankove, *Absorption, in: Optical Processes in Semiconductors*, Dover Publications, New York, NY, 1971, p. 34.
- [35] E. Shpiro, V. Avashev, G. Antoshin, M. Ryashentseva, K.M. Minachev, *J. Catal.* 55 (1978) 402–406.